

TEXTURE SEGMENTATION USING OVERCOMPLETE-WAVELET-FRAME BASED FRACTAL SIGNATURES

Li-Chang Liu, Jong-Chih Chien, and C. C. Li

Department of Electrical Engineering
University of Pittsburgh
Pittsburgh, PA 15261, USA

Email: {lilst4+,jocst4+}@pitt.edu, ccl@vms.cis.pitt.edu

ABSTRACT

This paper presents a variation of the wavelet-based fractal signature recently developed by Espinal, Huntsberger et al. Here, the overcomplete-wavelet-frame, instead of the standard wavelet basis, is used as multiscale signal/image representation to enhance the textural characterization by fractal signatures derived therefrom. Experimental results have demonstrated that this approach can improve texture representation and enable better detection of texture boundaries.

I. INTRODUCTION

Textures are repetitive visual patterns for surfaces of objects and provide important information for object segmentation and identification. The traditional statistical image texture analysis is concerned with the spatial interaction of pixel intensities over a certain neighborhood. Local features may be extracted from the co-occurrence of pixel intensities at specified neighboring positions relative to each pixel in the image. Statistics may be taken on such measurements to provide a texture description. Segmentation of a textured image is a difficult task, in particular, the accurate texture boundary determination. Recent research on human vision suggests the plausible modeling of Gabor filtering or wavelet filtering which may provide the joint space/frequency resolution. Multichannel filtering with different scale and orientation tuning is able to provide localized spatial changes in frequency [1]; however, outputs of the Gabor filter bank are not mutually orthogonal which may lead to significant correlation among texture features. On the other hand, wavelet transform provides a unifying framework for multiresolution analysis and can be applied to texture analysis and segmentation [2-9]. Unser [6] and Laine [7] introduced the use of wavelet frames for representing texture characteristics, and extracted features from the wavelet channels for texture classification and segmentation. Hsin et al. [8] used modulated wavelets for providing both spatial frequency and orientation selectivity in texture segmentation. More recently,

Espinal et al. [9] used wavelet-based fractal signatures as a texture measure for recognition and segmentation. They have show its capability to distinguish texture boundaries. In this paper, we evaluate fractal signatures based on overcomplete-wavelet-frame representation of a textured image with a goal to enhance their texture characterization and localization. Our experimental results on sample images have shown that this method can improve texture segmentation and provide better detection of texture boundaries. In the following section, we will give a brief review of wavelet transforms and wavelet frames. We will then discuss the overcomplete-wavelet-frame based fractal signatures.

II. WAVELET BASIS AND WAVELET FRAMES

Wavelet Transform

Wavelet transform is used as a new methodology for multiscale representation of all finite energy signals, that is, signal $f(x)$ in function space $L^2(\mathbb{R})$. A wavelet $\psi(x)$ is a small wave satisfying certain conditions such as having zero mean value and decaying rapidly toward zero (e.g., compactly supported). When $\psi(x)$ is dilated with a dyadic scale 2^j and translated in integer units n ,

$$\psi_{j,n}(x) = 2^{-j/2} \psi(2^{-j}x - n),$$

the set $\{\psi_{j,n}(x)\}$ forms a basis spanning a subspace W_j . Corresponding to $\psi(x)$, there is a scaling function $\phi(x)$ related to $\psi(x)$ via

$$\psi(x) = 2 \sum_k g(k) \phi(2x-k).$$

$\phi(x)$ satisfies a 2-scale dilation equation

$$\phi(x) = 2 \sum_k h(k) \phi(2x - k).$$

$\phi(x)$ can be similarly dilated and translated

$$\phi_{j,n}(x) = 2^{-j/2} \phi(2^{-j}x-n)$$

and the set $\{\phi_{j,n}(x)\}$ forms a basis spanning a subspace V_j . Any function in the respective subspace can be represented as a linear combination of these basis functions. Let A_j be a projection operator which projects a function $f(x)$ in $L^2(R)$ into the subspace V_j , that is, it approximates $f(x)$ by $f_j(x)$ at resolution 2^j , where $j \in Z$ (a set of integers). A multiresolution analysis is a set of spaces $(V_j)_{j \in Z}$ that satisfy the following properties:

$$(1) \dots \subset V_3 \subset V_2 \subset V_1 \subset V_0 \subset V_{-1} \subset V_{-2} \subset V_{-3} \subset \dots$$

, which means that an approximation at a higher resolution contains all the information in a lower resolution;

$$(2) f_j(x) \in V_j \leftrightarrow f_j(2x) \in V_{j-1};$$

$$(3) \overline{\bigcup_{j \in Z} V_j} = L^2(R), \quad \bigcap_{j \in Z} V_j = \emptyset,$$

The approximation $f_{j-1}(x)$ in V_{j-1} is further approximated by $f_j(x)$ in V_j with approximation error represented in W_j , so W_j is a complement to V_j in V_{j-1} and $V_{j-1} = V_j \oplus W_j$.

Compactly supported orthogonal wavelets have been constructed by Daubechies such that $\{\phi_{j,k}(x)\}_{k \in Z}$ forms an orthonormal basis for V_j . $\{\psi_{j,k}(x)\}_{k \in Z}$ forms an orthonormal basis for W_j , and $W_j \perp V_j$. If we stop at a scale level $j=J$, $f(x)$ can be represented by the following description

$$f(x) = \sum_k c_{j,k} \phi_{j,k}(x) + \sum_{j=J}^{\infty} \sum_k d_{j,k} \psi_{j,k}(x).$$

where the scaling coefficients $c_{j,n}$ and wavelet coefficients $d_{j,n}$ can be computed by

$$c_{j,n} = \sum_k h(k-2n)c_{j-1,k}$$

$$d_{j,n} = \sum_k g(k-2n)c_{j-1,k}$$

For the biorthogonal multiresolution analysis, the function space $L^2(R)$ is described with two different series of embedded subspaces, one is dual to the other,

$$\dots V_{j+1} \subset V_j \dots \quad \dots \tilde{V}_{j+1} \subset \tilde{V}_j \dots, \quad \tilde{V}_j \text{ is the dual of } V_j$$

$$\overline{\bigcup_{j \in Z} V_j} = L^2(R), \quad \bigcap_{j \in Z} V_j = \emptyset,$$

$$\overline{\bigcup_{j \in Z} \tilde{V}_j} = L^2(R), \quad \bigcap_{j \in Z} \tilde{V}_j = \emptyset,$$

V_j and \tilde{V}_j are spanned by sets of scaling functions $\{\phi_{j,n}\}$ and $\{\tilde{\phi}_{j,n}\}$, respectively. Similarly, there are complementary subspaces W_j and \tilde{W}_j , dual to each other, spanned by sets of corresponding wavelets $\{\psi_{j,n}(x)\}$ and $\{\tilde{\psi}_{j,n}\}$, respectively. Wavelets $\psi(x)$ and $\tilde{\psi}(x)$ are dual to each other, so that

$$\langle \psi_{m,q}(x), \tilde{\psi}_{j,k}(x) \rangle = \delta_{m,n} \delta_{q,k}$$

The orthogonality holds only between dual subspaces, i.e.,

$$V_{j-1} = V_j \oplus W_j, \quad \tilde{V}_{j-1} = \tilde{V}_j \oplus \tilde{W}_j$$

$$V_j \perp \tilde{W}_j, \quad \tilde{V}_j \perp W_j, \quad \text{and } \tilde{W}_j \perp W_k \text{ for } j < k$$

Any function $f(x) \in L^2(R)$ can be represented as

$$f(x) = \sum_j \sum_q \langle \tilde{\psi}_{j,q}(x), f(x) \rangle \psi_{j,q}(x)$$

where $\langle -, - \rangle$ denotes the inner product. If f_0 is the projection of $f(x)$ in V_0 and the decomposition is stopped at the scale level J , then

$$\begin{aligned} f_0(x) &= \sum_q \langle \tilde{\phi}_{j,q}(x), f(x) \rangle \phi_{j,q}(x) + \sum_{j=J}^1 \sum_k \langle \tilde{\psi}_{j,k}(x), f(x) \rangle \psi_{j,k}(x) \\ &= \sum_k c_{j,k} \phi_{j,k}(x) + \sum_{j=J}^1 \sum_k d_{j,k} \psi_{j,k}(x) \end{aligned}$$

$$\text{with } c_{j,k} = \langle \tilde{\phi}_{j,k}(x), f(x) \rangle, \quad d_{j,k} = \langle \tilde{\psi}_{j,k}(x), f(x) \rangle.$$

The scaling coefficients and wavelet coefficients in the decomposition are recursively computed by

$$c_{j,k} = \sum_q \tilde{h}(q-2k)c_{j-1,q}$$

$$d_{j,k} = \sum_q \tilde{g}(q-2k)c_{j-1,q}$$

where $\{\tilde{h}(n)\}$ and $\{\tilde{g}(n)\}$ are the low-pass and high-pass decomposition filters, respectively. Note that $\tilde{h}(n)$ and $\tilde{g}(n)$ are derived from the dual scaling function

$\tilde{\phi}(x)$ and dual wavelet $\tilde{\psi}(x)$ instead of the decomposition scaling function $\phi(x)$ and wavelet $\psi(x)$.

In practical applications to digital signals and images, $f(x)$ is not known; we use the original digital data as $\{c_{0,k}\}$. For applications to digital images, the 2-D wavelet transform can be implemented by a tensor product of two 1-D wavelet transforms: first along the row direction, and then along the column direction. An image of size $n \times n$ is decomposed at the first scale level to four subimages, each is downsampled to size $\frac{n}{2} \times \frac{n}{2}$, consisting of one scaling subimage denoted as LL (low-pass filtered both horizontally and vertically) and three wavelet subimages denoted as HL (low-pass filtered horizontally and high-pass filtered vertically), LH (high-pass filtered horizontally and low-pass filtered vertically), and HH (high-pass filtered both horizontally and vertically). The scaling subimage is to be further decomposed to the next scale level, etc.

Overcomplete Wavelet Frames

The set of scaled and translated decomposition wavelets $\{\psi_{b,j,k}\}$ form a frame,

$$\psi_{b,j,k}(x) = 2^{-j/2} \psi(2^{-j}x - kb),$$

if there exist positive constants A and B, with $0 < A \leq B < \infty$, such that

$$A\|f\|^2 \leq \sum_{j,k} \left| \langle f, \psi_{b,j,k} \rangle \right|^2 \leq B\|f\|^2$$

holds for all $f(x) \in L^2$, where b denotes the translation unit at scale j, $\|f\|^2 = \langle f, f \rangle$ measures the energy of signal $f(x)$. A and B are called frame bounds of the frame $\{\psi_{b,j,k}\}$. If $A=B$, then the frame is called a tight frame, i.e., a set of complete and independent basis. Every tight frame $\{\psi\}$ has a dual given by $\tilde{\psi} = \frac{1}{A} \psi$, then

$$f(x) = \frac{1}{A} \sum_{j,k \in \mathbb{Z}} \langle f, \psi_{j,k} \rangle \psi_{j,k}, \quad f \in L^2$$

When A is equal to 1, the frame becomes an orthogonal basis. Frames may contain redundancy, oversampled frames generate redundant frames. If $b=2^j$, $\psi_{b,j,k}(x)$ represents a dilated $\psi(x)$ with scale 2^j but translated by k units in the original scale; this set $\{\psi_{b,j,k}(x)\}$ is called the overcomplete wavelet frame. Wavelet coefficients obtained in wavelet decomposition without downsampling are wavelet coefficients of the

overcomplete-wavelet-frame decomposition. They are computed by

$$c_{j,k} = \sum_n \tilde{h}(n) c_{j-1,k+2^{j-1}n}$$

$$d_{j,k} = \sum_n \tilde{g}(n) c_{j-1,k+2^{j-1}n}$$

When the orthogonal wavelet transform is considered, $h(n)$ and $g(n)$ will be used in the above equation. Since they are available at all pixels, they provide more localized information for all scales even though they contain some redundant information. This is utilized in multiscale edge detection [3] and also in texture analysis [6]. We will examine fractal signatures based on the overcomplete-wavelet-frame decomposition.

III. OVERCOMPLETE-WAVELET-FRAMES BASED FRACTAL SIGNATURES

Fractal is a mathematical model describing the scaling or self similarity property in geometry. Fractal dimension is defined as a measure of roughness (or smoothness) of a surface. If $f(x)$ is a graph over a unit interval of x and the interval is divided into 2^v subintervals, let us attempt to cover the graph with $N(v,f)$ elementary squares of side length 2^{-v} (or balls of diameter 2^{-v}). The fractal dimension of a graph is given by

$$\dim(f) = \lim_{v \rightarrow \infty} \frac{\log N(v, f)}{\log \frac{1}{2^{-v}}} = \lim_{v \rightarrow \infty} \frac{\log N(v, f)}{\log 2^v}$$

The scaling by 2^{-v} as $v \rightarrow \infty$ will reveal the roughness of f in variation over the interval. The notion of fractal dimension may be applied to wavelet subimages to characterize certain texture information in an original image f, since wavelet components of an image reflect the high frequency information on the surface [9,10,11]. Instead of counting the number $N(v,f)$ of elementary volumes which cover the wavelet surface, one can compute the sum of absolute amplitudes of wavelet coefficients $W_{v,\theta}(f)$ at the scale level (-v) on sub-samples of spatial resolution $2^{-v} \times 2^{-v}$ over a unit area. Here $\theta=1, 2, 3$ denote the horizontal, vertical and diagonal channels, respectively. Thus [9]

$$\dim[\text{graph}(f)] = \lim_{v \rightarrow \infty} \frac{\log^+ \left\{ \sum_{A=2^{-2v}} |W_{v,\theta}(f)| A^{-1/2} \right\}}{\log^+ 2^v} + 1$$

where A is the elementary area $2^{-v} \times 2^{-v}$ at the scale level (-v), $\log^+(y) = \max(\log y, 0)$ for $y > 0$ and $\log^+(y) = 0$ for $y = 0$, and the summation is taken over the unit area in the original scale (level 0).

Wavelet-Based Fractal Signature

In practical situations, one can not compute wavelet coefficients $W_{j,\theta}$ at the infinitely fine resolution (scale level $-\infty$). Instead, one can use fractal signatures $D_{j,\theta}$ at each pixel ($j=1,2,\dots,J; \theta=1,2,3$) defined by [9]

$$D_{j,\theta} = \frac{\log^+ \left\{ \sum_{N(P)} |W_{j,\theta}| \sqrt{2^{-2j}} \right\}}{\log^+ (2^j)}$$

where the summation of $|W_{j,\theta}|$'s is taken over a neighborhood $N(P)$ of $m \times m$ pixels around each pixel P and $j=1, 2, \dots, \log_2 m$.

Overcomplete-wavelet-frame Based Fractal Signatures

We propose to evaluate fractal signatures on wavelet subimages from the overcomplete wavelet frame decomposition. In this case, wavelet coefficients $W_{j,\theta}$ at any pixel location for all scale levels $j \geq 1$ are readily available, these signatures extract more localized information at each scale even though the computation involves some redundant information. When used as texture features in texture segmentation, they may help to provide improved texture boundaries. Note that the summation term in the numerator of $D_{j,\theta}$ is equivalent to the windowed mean of wavelet frame coefficients used by Unser [6]. The fractal signature modifies the windowed mean by a factor depending upon the scale. We will explore the potential merit of these fractal signatures in experiments discussed in the following.

IV. EXPERIMENTS ON TEXTURE SEGMENTATION

Texture segmentation experiments were performed on two images: (1) a composite of four Brodatz images (128x128 pixels) shown in Figure 2, and (2) a cloud image (360x300 pixels) shown in Figure 6. Biorthogonal wavelet Bior 2.2 (in Matlab) and Daubechies' orthogonal wavelet Daubech3 were used, decomposition scaling functions and wavelets are shown in Figure 1. Decomposition filter coefficients are given by:

Bior 2.2

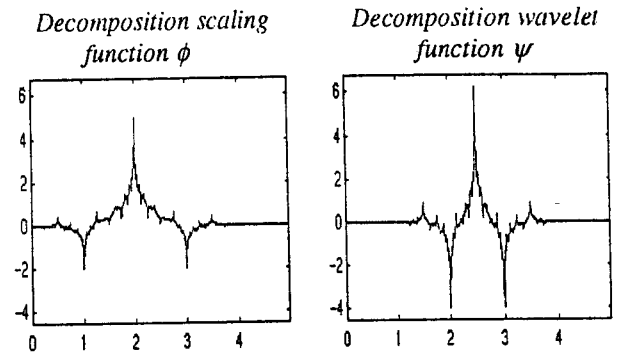
$$\{\tilde{h}(n)\} = [-0.1768 \ 0.3536 \ 1.0607 \ 0.3536 \ -0.1768]$$

$$\{\tilde{g}(n)\} = [0.3536 \ -0.7071 \ 0.3536]$$

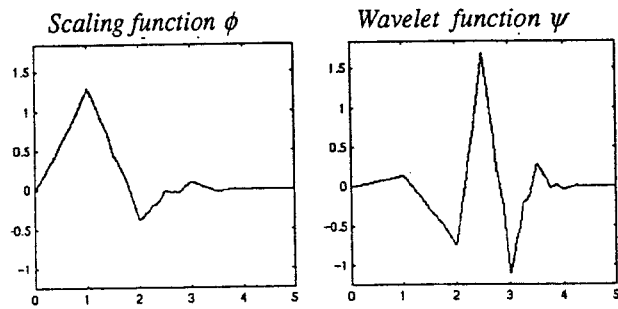
Daubech3

$$\{h(n)\} = [0.0352 \ -0.0854 \ -0.1350 \ 0.4599 \ 0.8069 \ 0.3327]$$

$$\{g(n)\} = [-0.3327 \ 0.8069 \ -0.4599 \ 0.0854 \ 0.0352]$$



(a) Bior 2.2 scaling function and wavelet



(b) Daubech3 scaling function and wavelet

Figure 1. Scaling functions and wavelets used in our experiments.

Decomposition up to level 2 were considered. Using selected texture features, the fuzzy C-means clustering algorithm was applied for texture segmentation,

A Composite of Four Brodatz Images

In this experiment, first, we compared segmentation results obtained by using three different sets of features: (1) overcomplete-wavelet-frame based fractal signatures, (2) wavelet-based fractal signatures of Espinal et al., and (3) windowed means in wavelet-frame decomposition used by Unser (but without further extraction with Karhonen-Loeve transformation). The biorthogonal wavelet Bior 2.2 was used and only the first level of decomposition was considered. Since only fine textures are included in the whole image, we chose a small window size of 8x8. The ground truth about the four textures in the composite image was known, so the segmentation results were evaluated by computing the correct classification rate in each case, as shown in Table 1. Using fractal signatures based on wavelet-frame coefficients (see Figure 3 and Table 1) improved the segmentation result in comparison to using fractal signatures based on the standard wavelet coefficients (Figure 4 and Table 1). When compared to the case of windowed means of wavelet-frame coefficients (see Figure 5 and Table 1), it also gave better performance with a small gain in classification rate. This observation suggests that the overcomplete-wavelet-frame decomposition has merits in texture feature extraction.

Table 1: Experimental results of texture segmentation of the image in Figure 2 using three different sets of features extracted on the first level of wavelet decomposition.

	Decomp. Filter	Window size	Classif. rate
Wavelet-based fractal signature	Bior (2,2)	8x8	73.34%
Windowed mean in wavelet-frame decomposition	Bior (2,2)	8x8	89.00%
Wavelet-frame-based fractal signature	Bior (2,2)	8x8	90.72%

Second, using the overcomplete-wavelet-frame decomposition approach, we compared the performances of Bior2.2 and Daubech3 in texture segmentation, and also examined the effect of using reduced samples in computing second level fractal signatures, as show in Table 2. Bior2.2 gave a better performance. Using skip sampling at scale level 2, only $\frac{1}{4}$ of the wavelet-frame

coefficients were used in evaluating $D_{2,0}$, the resulting classification rate was essentially the same. This suggests a possible saving in computation time, but maintaining the improved performance in texture segmentation.

A Cloud Image

A cloud image (360x300 pixels) in Figure 6 shows a part of a remotely sensed image of clouds over the North Sea. This image was experimented before by Hsin [8] for texture segmentation with modulated wavelets. A spread of cold air is on the left, and cloud streets of a cyclone appears on the right. Three texture classes were assumed to exist: cyclone cloud streets, cold air, and the rest (including sea and land). We used the biorthogonal (Bior 2.2) wavelet frame decomposition and selected six wavelet-frame based fractal signatures at the first two resolution levels, $D_{1,1}$, $D_{1,2}$, $D_{1,3}$, $D_{2,1}$, $D_{2,2}$, and $D_{2,3}$. The window size was 32x32. The clustering algorithm was applied to segment the image into three texture classes as shown in Figure 7(a), the determined texture boundaries were overlaid on the original image as shown in Figure 7(b). This result is better than what was attained in Ref. [8]. We also noticed that the addition of fractal signatures at scale level 2 improved the texture segmentation when

Table 2: Experimental results on texture segmentation of the image in Figure 2 using overcomplete-wavelet-frame fractal signatures extracted on the first two levels of wavelet decomposition.

Decomp. Filter	Method	Window size	Classif. rate
Bior (2,2)	Fully over-sampled	8x8	90.93%
Bior (2,2)	Skip sampling at level 2.	8x8	91.00%
Daubech3	Fully over-sampled	8x8	87.46%
Daubech3	Skip sampling at level 2	8x8	87.45%

compared to the result obtained by using fractal signatures at scale level 1 only.

V. CONCLUSION

We have introduced a variation of wavelet-based fractal signatures for texture segmentation by evaluating fractal signatures on wavelet coefficients of the overcomplete wavelet frame decomposition. The coefficients for all scales ($j=1, 2, \dots, J$) are readily available at every pixel in this image, the computation of fractal signatures at all scales becomes more convenient and more localized in comparison to the standard wavelet-based fractal signatures. Experimental results have shown their improved performance on multiscale texture segmentation.

ACKNOWLEDGEMENT

The authors would like to thank Professor D. J. Hebert, Department of Mathematics, University of Pittsburgh, for his suggestions and helps in this research.

VI. RERENCES

- [1] A. K. Jain and F. Farrokhnia, "Unsupervised texture segmentation using Gabor filters," Pattern Recognition., Vol. 24, pp. 1167-1186, Dec. 1991.
- [2] M. Unser and M. Eden, "Multiresolution feature extraction and selection for texture segmentation," IEEE Trans. Pattern Anal. Mach. Intell., Vol. 11, no. 7, pp. 717-728, 1989.

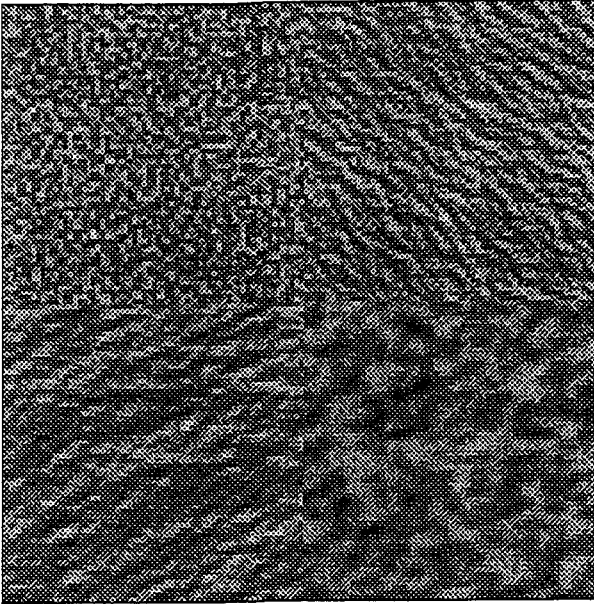


Figure 2: A composite of four Brodatz images (128x128 pixels).

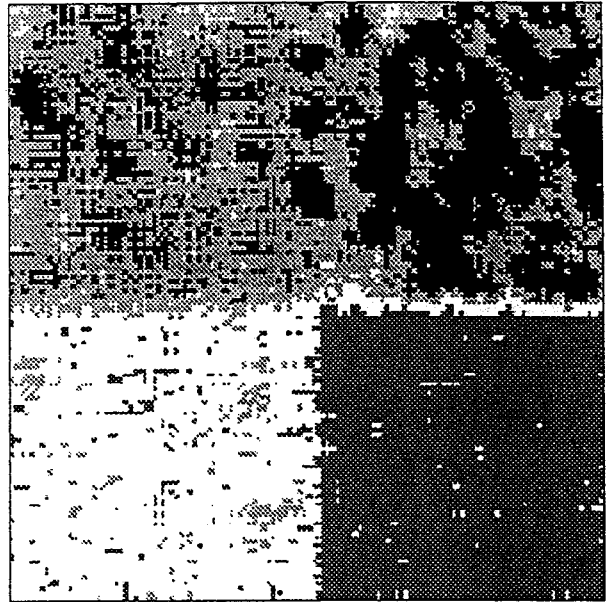


Figure 4. Texture segmentation of the image in Figure 2 obtained by using wavelet-based fractal signatures at the first decomposition level (Bior 2.2, window size 8 x 8, classification rate 73.34%).

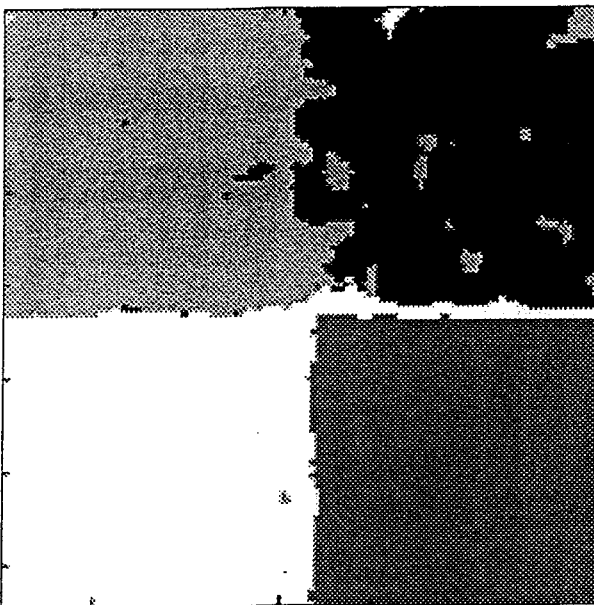


Figure 3. Texture segmentation of the image in Figure 2 obtained by using overcomplete-wavelet-frame based fractal signatures at the first decomposition level (Bior. 2.2, window size 8 x 8, classification rate 90.72%)

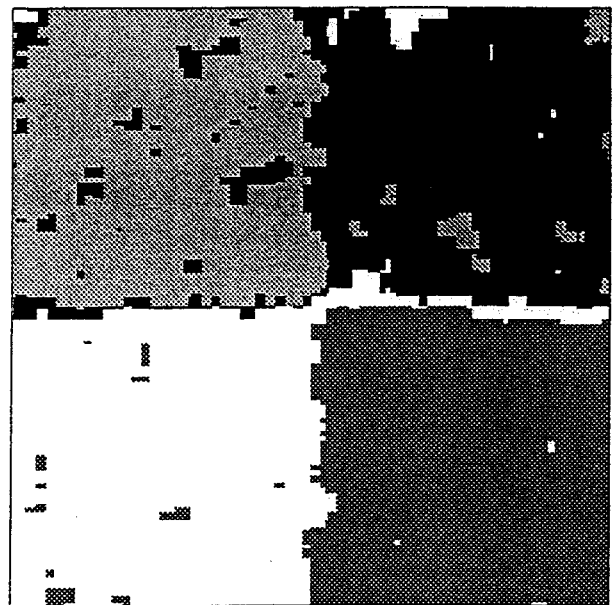


Figure 5. Texture segmentation of the image in Figure 2 obtained by using windowed means in three orientation channels at the first level of wavelet-frame decomposition. (Bior 2.2, window size 8 x 8, classification rate 89.00 %).

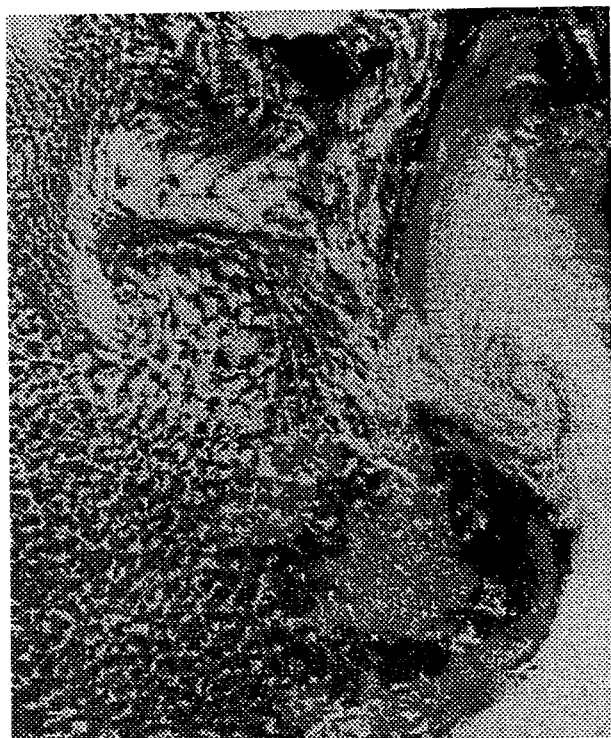
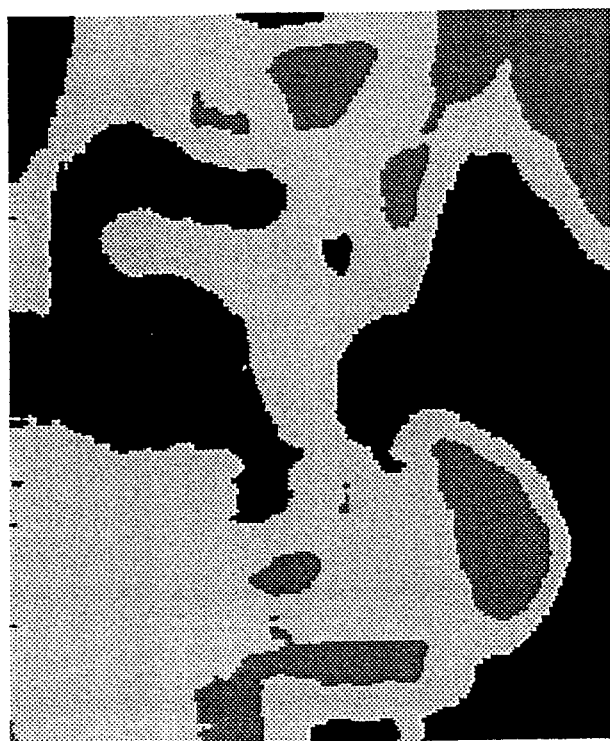


Figure 6. An original cloud image, (360 x 300 pixels)



(a) Segmentation into three texture classes



(b) The original cloud image with an overlay of the segmented texture boundary.

Figure 7. Texture segmentation of the cloud image in Figure 6 obtained by using the overcomplete-wavelet-frame based fractal signatures at the first two decomposition levels. (Bior 2.2, window size 32 x 32),

- [3] S. Mallat, "A Theory for Multiresolution signal decomposition: the wavelet representation," *IEEE Trans. Pattern Anal. Mach. Intell.*, Vol. 11, pp. 674-693, 1989.
- [4] T. Chang and C.C.J. Kuo, "Texture analysis and classification with tree-structured wavelet transform," *IEEE Trans. Image Processing*, Vol. 2, no. 4, pp. 429-441, Oct. 1993.
- [5] A. Laine and J. Fan, "Texture classification by wavelet packet signatures," *IEEE Trans. Pattern Anal. Mach. Intell.*, Vol. 15, no. 11, pp. 1186-1191, Nov. 1993.
- [6] M. Unser, "Texture classification and segmentation using wavelet frames," *IEEE Trans. Image Processing*, Vol. 4, no. 11, pp. 1549-1560, Nov. 1995.
- [7] A. Laine and J. Fan, "Frame representation for texture segmentation," *IEEE Trans. Image Processing*, Vol. 5, pp. 771-780, May 1996.
- [8] H.C. Hsin and C.C. Li, "An experiment on texture segmentation using modulated wavelets," *IEEE Trans. Systems, Man and Cybernetics, Part A*, Vol. 28, No. 4, Aug. 1998.
- [9] F. Espinal, T. Huntsberger, B. D. Jawerth, and T. Kubota, "Wavelet-based fractal signature analysis for automatic target recognition," *Optical Engineering*, Vol. 37, no. 1, pp. 166-174, Jan. 1998.
- [10] A. Deliu and B. Jawerth, "Geometrical dimension versus smoothness," *Construct. Approx.*, Vol. 8, pp. 211-222, 1992.
- [11] F. Argoul, A. Arneodo, J. Elezgaray, and G. Grasseu, "Wavelet transform of fractal aggregates," *Phys. Lett. A*, Vol. 135, 6/7, pp. 327-335, 1989.